First-principles calculation of nitrogen-tungsten codoping effects on the band structure of anatase-titania

Run Long and Niall J. English[a)]

The SEC Strategic Research Cluster and the Centre for Synthesis and Chemical Biology, Conway Institute of Biomolecular and Biomedical Research, School of Chemical and Bioprocess Engineering, University College Dublin, Belfield, Dublin 4, Ireland

The electronic properties and photocatalytic activity of nitrogen (N) and/or tungsten (W)-doped anatase are calculated using density functional theory. For N-doping, isolated N 2p states above the top of the valence band are responsible for experimentally observed red-shifts in the optical absorption edge. For W-doping, W 5d states below the conduction band lead to band gap narrowing; the transition energy is reduced by 0.2 eV. Addition of W to the N-doped system yields significant band gap narrowing gap by 0.5 eV. This rationalizes recent experimental data which showed that N/W-doped titania exhibits higher visible-light photocatalytic efficiency than either N- or W-doping alone.

Keywords: N/W-doped, electronic structure, TiO_2

[a)] Corresponding author. Electronic Mail: niall.english@ucd.ie

Titania (TiO_2) has received intense attention as a promising photocatalytic material for years [1, 2]. However, as a wide band gap semiconductor (3.20 eV), anatase allows only absorption of ultraviolet irradiation, which amounts to ~5% of solar energy. Further, its photoexcited electron-hole pairs recombine relatively easily. To extend optical absorption of TiO_2-based materials to the visible-light region, doping with metals and nonmetals [3-12] has been used widely. However, reported studies of codoping with both metal and nonmetal elements are very rare. N-doped TiO_2 is considered to be one of the most effective photocatalysts and it has been investigated widely, both by experimental and theoretical methods [9]. However, the nature of N-induced modifications to the electronic band structure depends on the doping content. Either band gap narrowing [9] or formation of localized midgap states [10] have been proposed for red-shifts of the optical absorption edge. Asahi et al. [9] concluded from first-principles calculations that N atoms were substituted for lattice O atoms causing narrowing of the band gap by mixing of N 2p and O 2p states. Conversely, Irie et al. [10] have suggested that the visible-light response in N-doped TiO_2 may be due to N 2p states isolated above the valence band maximum. In principle, WO_3 coupling has been used widely to improve the photocatalytic performance of TiO_2, because it reduces the recombination of electron-hole pairs [14] and expands the range of useful excitation radiation to the visible region. Recently, many experiments have focused on the addition of W to N-doped TiO_2 to increase photocatalytic activity under visible light irradiation [15, 16]. However, there have been no previous reports of theoretical studies to investigate the origin of visible light

photocatalytic activity in N/W-codoped TiO_2, or for the single W-doped TiO_2 case.

This study focuses on the energetic and electronic structure of doped anatase using density functional theory (DFT) calculations, and rationalizes the origin of experimentally observed red-shifts in the optical absorption edge and synergetic effects of N/W-codoping. We also discuss the thermodynamic properties of N-, W-, and N/W -doped TiO_2 from analysis of calculated formation energies.

All of the spin-polarized DFT calculations were performed using the projector augmented wave (PAW) pseudopotentials as implemented in the Vienna ab initio Simulation Package (VASP) code [17, 18]. The Perdew and Wang parameterization [19] of the generalized gradient approximation (GGA) [20] was adopted for the exchange-correlation potential. The electron wave function was expanded in plane waves up to a cutoff energy of 400 eV and a Monkhorst–Pack *k*-point mesh [21] of 4 × 4 × 4 was used for geometry optimization [22, 23] and electronic property calculations. The optimized lattice parameters for pure anatase were found to be a = 3.800 Å and c = 9.483 Å, in good agreement with experimental and other theoretical results [24, 25], indicating that our methodology is reasonable.

The doped systems were constructed from a relaxed (2 × 2 × 1) 48-atom anatase supercell. The N atom was substituted for O atoms and the W atom was substituted for Ti atoms. N/W-doped TiO_2 was modeled by single substitution of N for one O atom, and its adjacent Ti atom was replaced by one substitution of an W atom per supercell, because calculations show that the formation of an adjacent pair of N and W is energetically favorable by 0.57 eV vis-à-vis other N-W configurations; this

finding is supported by Raman and X-ray diffraction (XRD) measurements [16]. The supercell system is shown in Fig. 1.

To determine systems' relative stability, we calculated dopant formation energies; these may be viewed as the relative difficulty for different ions to incorporate into anatase, and is a widely accepted gauge of energetic stability. The formation energies of substitutional dopant defects are

$$E_{form} = E(doped) - E(pure) - \mu_N - \mu_W + \mu_O + \mu_{Ti} \quad (1)$$

where $E(doped)$ is the total energy of the system containing the N, W, or N/W impurity and $E(pure)$ is the total energy of the pure host supercell. μ_N and μ_W are the chemical potentials of the N and W impurities, respectively; μ_O (μ_{Ti}) is that of O (Ti). The formation energy depends on growth conditions, which may be varied from Ti- to O-rich. For TiO_2, μ_O and μ_{Ti} satisfy the relationship $\mu_{Ti} + 2\mu_O = \mu(TiO_2)$. Under O-rich conditions, μ_O is determined by the energy of an O_2 molecule ($\mu_O = \mu(O_2)/2$) and μ_{Ti} is determined from the formula above. Under Ti-rich conditions, μ_{Ti} amounts to the energy of one Ti atom in bulk Ti ($\mu_{Ti} = \mu_{Ti}^{metal}$) and then μ_O is calculated on the basis of the above formula. For dopants, μ_N is determined from $\mu_N = \mu(N_2)/2$ and μ_W is calculated from bulk metal tungsten ($\mu_W = \mu_W^{metal}$). The calculated formation energies are summarized in Table 1. Their order suggests that: 1) N occupies the O site preferentially under Ti-rich conditions; 2) W is substituted preferentially for Ti under O-rich conditions; 3) the incorporation of N promotes that of W under both Ti- and O-rich conditions. Therefore, the experimental synthesis of N/W-doped TiO_2 is more thermodynamically

favorable vis-à-vis single W doping under Ti-rich conditions, due to a lower formation energy of 1.61 eV. Further, both single W doping and N/W-codoping are energetically favorable under O-rich conditions due to negative formation energies.

To compare modifications in the band structure and the origin of red-shifts in the absorption light edge with different doping configurations, we calculated the density of states (DOS) and the projected density of states (PDOS); these are plotted in Fig. 2. The calculated band gap of pure anatase is 2.0 eV, as shown in Fig. 2a, which is similar to other theoretical results [11], but underestimates the experimental value of 3.20 eV, due to well-known limitations in DFT. However, in this study, we focus on changes in the band gap upon doping, so the GGA method is expected to largely cancel the band gap error between different systems. Further, recent theoretical work focused on nonmetal codoping with transition metals has shown that standard DFT methods can deal fully with these doped systems [26]. For N-doped TiO_2 (Figs. 2b & f), an O atom is replaced by an N atom, leaving the system deficient by one electron. This implies that the N oxidation state is -2 rather than -3, and that its 2p states are not fully occupied, giving the N atom a doublet spin state. It is clear in Fig. 2 that N 2p states are localized in the band gap without altering the valence band maximum (VBM) and conduction band minimum (CBM) vis-à-vis the undoped case. The electron in the valence band can be excited into gap states and then subsequently to the conduction band by visible-light absorption, suggesting that gap-to-conduction band transitions are responsible for red shifts in the absorption edge. Conversely, emptied N 2p states can act as traps for excited electrons, which can serve to promote

electron-hole recombination rates. Therefore, the photocatalytic activity of N-doped TiO_2 is more limited in the visible light region. For W-doped TiO_2 (Figs. 2c & g), the impurity states lie below the CBM, indicating that W 5d states are below host Ti 3d states. This led to a band gap reduction by about 0.2 eV. These states would be expected to lead to enhancements in photocatalytic efficiency. Indeed, doping by W may also be responsible for red-shifts in optical absorption edges observed experimentally [5, 6]. Figs. 2a & e shows that the valence band edge consists mainly of O 2p states, whereas the conduction band edge has predominately Ti 3d states. Therefore, codoping with N and W would be expected to modify the conduction and valence band edges simultaneously because N has a different atomic p orbital energy relative to O, and W has a different atomic d orbital energy vis-à-vis Ti. For N/W-doped TiO_2 (Figs. 2d & h), it is interesting that a hybridized state (composed of N 2p orbitals and W 5d states) is formed; in particular, the hybridized states are located mainly at the edge of the valence band whereas other W 5d states are at the edge of the conduction band. The W 5d states may contribute to the lowering of the energy levels of the N 2p states, bringing the N states closer to the valence band, and therefore enhancing mixing of N 2p and O 2p states in the valence band. In this case, the isolated states disappear and a continuum is formed. Conversely, the position of W 5d states were pushed to lower energy regions due to the interaction between W 5d and N 2p states, which led to a 0.5 eV reduction of the N/W band gap vis-à-vis pure TiO_2. It is clear that the addition of W to N-doped TiO_2 changes the character of N 2p orbitals from isolated midgap states to N 2p states mixed with O 2p states. As

electrons move from occupied W 5d states to empty lower energy 2p states (N^{2-} impurities), this indicates that N^{2-} ion (doublet) states transfer into N^{3-} ion (singlet) states, filling the 2p band. These results indicate clearly that N-W-O bonding leads to the formation of additional impurity states which can contribute to enhanced visible light absorption upon addition of W to N-doped TiO_2.

To study further the variation of N 2p impurity states with different behavior in the same N doping content in N- and N/W-doped TiO_2, we have plotted the total charge and spin density in Fig. 3. The inclusion of an N atom in the lattice results in a paramagnetic impurity and a doublet ground state. The unpaired electron has a strong N 2p character, and is largely localized on the N atom (Fig. 3a), with the spin density centered fully there (Fig. 3b). For N/W-doped TiO_2, however, the electron density is more localized on the N than W atom (Fig. 3c) while the spin density is very small and significantly dispersed. This shows that the spin density of an N atom couples with that of the adjacent W, resulting in hybridization of the N 2p with W 5d states (Figs. 2d & 3d]. This indicates that N forms a stable eight-electron shell with no unpaired electron because of Ti^{4+} replacement by W^{+6}. Bader charges [27, 28] are summarized in Table 2. They shows that the N ion has a charge of -1.37 |e| for N-doping, while it is -2.01 |e| for N/W-doping, with more electrons transferring from the W and adjacent Ti atoms to the N ion; this implies that the unpaired electron of N leads to the formation of a new bond with W. The bond length of N-W is 1.851 Å, which is much shorter than that of the N-Ti length of 2.026 Å for N-doping. This indicates further that a strong N-W bond forms in N/W-codoped TiO_2. These findings

helps to rationalize experimental reports of W doping leading to red-shifts in the optical absorption edge [5, 6] and N/W-codoping enhancing the absorption region and photocatalytic activity [15, 16].

In summary, we have calculated the electronic properties of N-, W-, and N/W-doped TiO_2 by DFT. The calculated results indicate that N and W codoping can reduce the band gap effectively and enhance photocatalytic activity under visible light irradiation. The hybridization between N 2p and W 5d states leads to strong mixing of N 2p and O 2p states, leading to the formation of continuum states. At the same time, W 5d states were located at the conduction band edge. Both of these factors led to band gap reduction, rationalizing experimental observations of enhanced photocatalytic activity.

This work was supported by the Irish Research Council for Science, Engineering and Technology.

References

[1] A. L.Linsebiger, G. Q. Lu, J. T.Yates, Chem. Rev. **95**, 725 (1995).

[2] A. Fujishima, K.Honda, Nature **28**, 37 (1972).

[3] J. M.Herrmann, J. Disdier, P. Pichat, Chem. Phys. Lett. **108**, 618 (1984).

[4] W.Choi, A. Termin, M. R. Hoffmann, J. Phys. Chem. **98**, 13669 (1984).

[5] N. Couselo, F. G. García, R. J. Candal, M. J. Jobbágy, Phys. Chem. C **112**, 1094 (2008).

[6] Y. Yang, H. Y. Wang, X. Li, C. Wang, Mater. Lett. **63**, 331 (2009).

[7] R. Long, Y. Dai, B. B. Huang, J. Phys. Chem. C **113**, 650 (2009).

[8] R. Long, Y. Dai, B. B. Huang, Comput. Mater. Sci. 2008, doi:10.1016/j.commatsci.2008.09.011

[9] R. Asahi, T. Morikawa, T. Ohwaki, K. Aoki, Taga, Y. Science **293**, 269 (2001).

[10] H. Irie, Y. Watanabe, K. Hashimoto, J. Phys. Chem. B **107**, 5483 (2003).

[11] T. Umebayashi, Y. Yamaki, H. Itoh, K. Asai, Appl. Phys. Lett. **81**, 454 (2002).

[12] D. Chen, D. Yang, Q. Wang, Y. Jiang, Ind. Eng. Chem. Res. **45**, 4110 (2006).

[13] S. Sakthivel, H. Kisch, Angew. Chem., Int. Ed. **42**, 4908 (2003)

[14] W. R. Duncan, O. V. Prezhdo, J. Am. Chem. Soc. **130**, 9756 (2008).

[15] B. F. Gao, Y. Ma, Y. A. Cao, W. S. Yang, J. N. Yao, J. Phys. Chem. B **110**, 14391 (2006).

[16] Y. F. Shen, T. Y. Xiong, T. F. Li, K. Yang, Applied Catalysis B: Enviormental **83**, 177 (2008).

[17] G. Kresse, J. Hafner, Phys. Rev. B **47**, 558 (1994).

[18] G. Kresse, J. Furtherműller, Phys. Rev. B **54**, 11169 (1996).

[19] J. P. Perdew, K. Burk, M. Ernzerhof, Phys. Rev. Lett. **77**, 3865 (1996).

[20] J. P. Perdew, Y. Wang, Phys. Rev. B **45**, 13244 (1992).

[21] H. J. Monkhorst, J. D. Pack, Phys. Rev. B **13**, 5188 (1976).

[22] E. R. Davidson, *Methods in Computational Molecular Physics* edited by G.H.F. Diercksen

[23] S. Wilson, Vol. 113 *NATO Advanced Study Institute, Series C* (Plenum, New York, 1983), p. 95.

[24] J. K. Burdett, T. Hughbandks, G. J. Miller, J. W. Richardson, J. V. Smith, J. Am. Chem. Soc. **10**, 3639 (1987).

[25] M. Lazzeri, A.Vittadini, A. Selloni, Phys. Rev. B **63**, 155409 (2001).

[26] Y. Q. Gai, J. B. Li, A. S. Li, J. B. Xia, S. H. Wei, Phys. Rev. Lett. **102**, 036402 (2009).

[27] G. Henkelman, A. Arnaldsson, H. Jónsson, Comput. Mater. Sci. **36**, 254 (2006).

[28] E. Sanville, S. D. Kenny, R. Smith, and G. Henkelman, J. Comp. Chem. **28**, 899 (2007).

Table 1. Formation energies (eV) E_{form} for N-, W-, and N/W-doped TiO_2.

		Ti-rich	O-rich
E_{form}	*N-doped*	*0.90*	*5.90*
E_{form}	*W-doped*	*3.40*	*-6.60*
E_{form}	*N/W-doped*	*1.61*	*-3.39*

Table 2 Bader Charges **(**|e|**)** on dopant atoms and their adjacent atoms in N-, W-, and N/W-doped TiO_2. The numbers in parenthesis represent the numbers of atoms.

	N-doped	W-doped	N/W-doped
N	*-1.37*		*-2.01*
W		*4.59*	*4.63*
O		*-1.47(2)*, *-1.49(2)*, *-1.58(2)*	*-1.36(2)*, *-1.49*, *-1.55 (2)*
Ti	*2.63(3)*		*2.60(2)*

Figure Captions

Figure 1. Supercell model for defective anatase TiO_2 showing the location of the dopants. The ion doping sites are marked with N and W. The large light spheres and the small dark spheres represent the Ti and O atoms, respectively.

Figure 2. DOS (left) for (a) pure TiO_2, (b) N-doped TiO_2, (c) W-doped TiO_2, and (d) N/W-doped TiO_2. The corresponding PDOS are shown on the right in (e)-(h). The PDOS plots of (f)-(h) are enlarged for clarity. The top of valence band of pure TiO_2 is taken as the reference level.

Figure 3 Electron densities (left) and spin densities (right). (a), (b) for N-doped TiO_2 and (c), (d) for N/W-doped TiO_2.

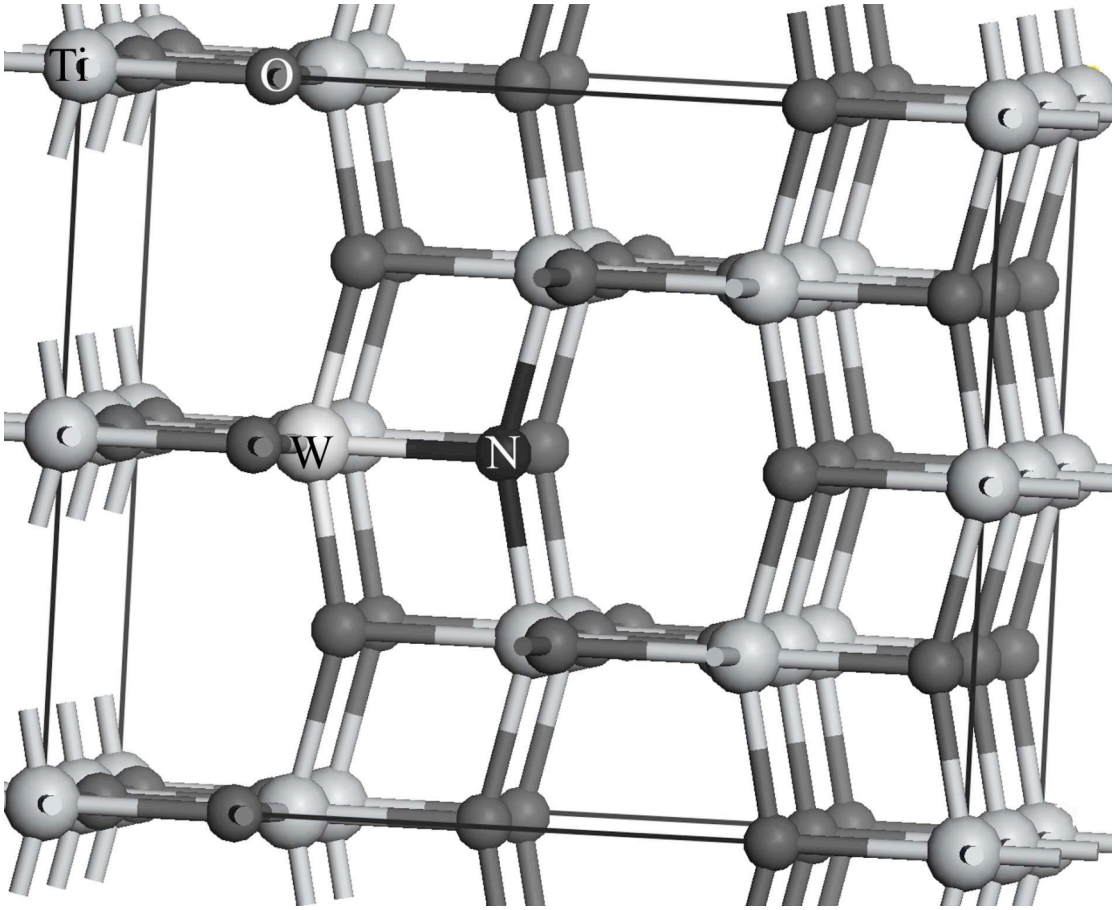

Figure 1

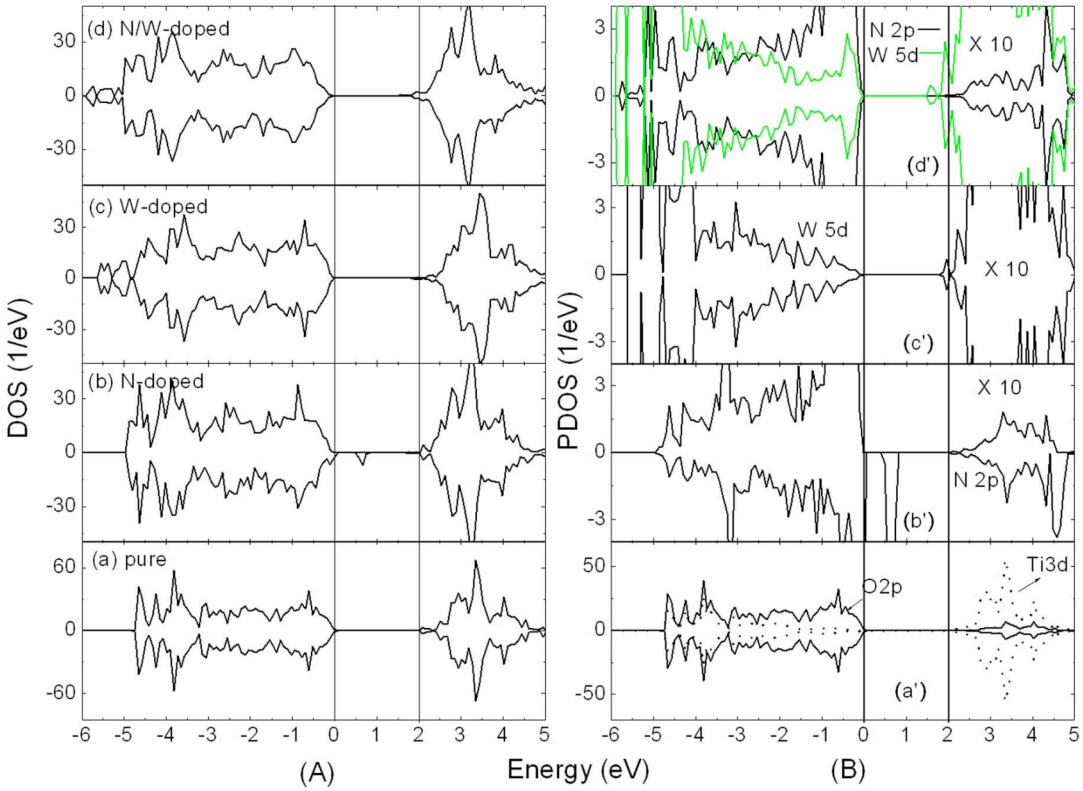
(d) N/W-doped
(c) W-doped
(b) N-doped
(a) pure
DOS (1/eV)
PDOS (1/eV)
N 2p
W 5d
X 10
(d')
(c')
(b')
(a')
O2p
Ti3d
(A)
Energy (eV)
(B)

Figure 2

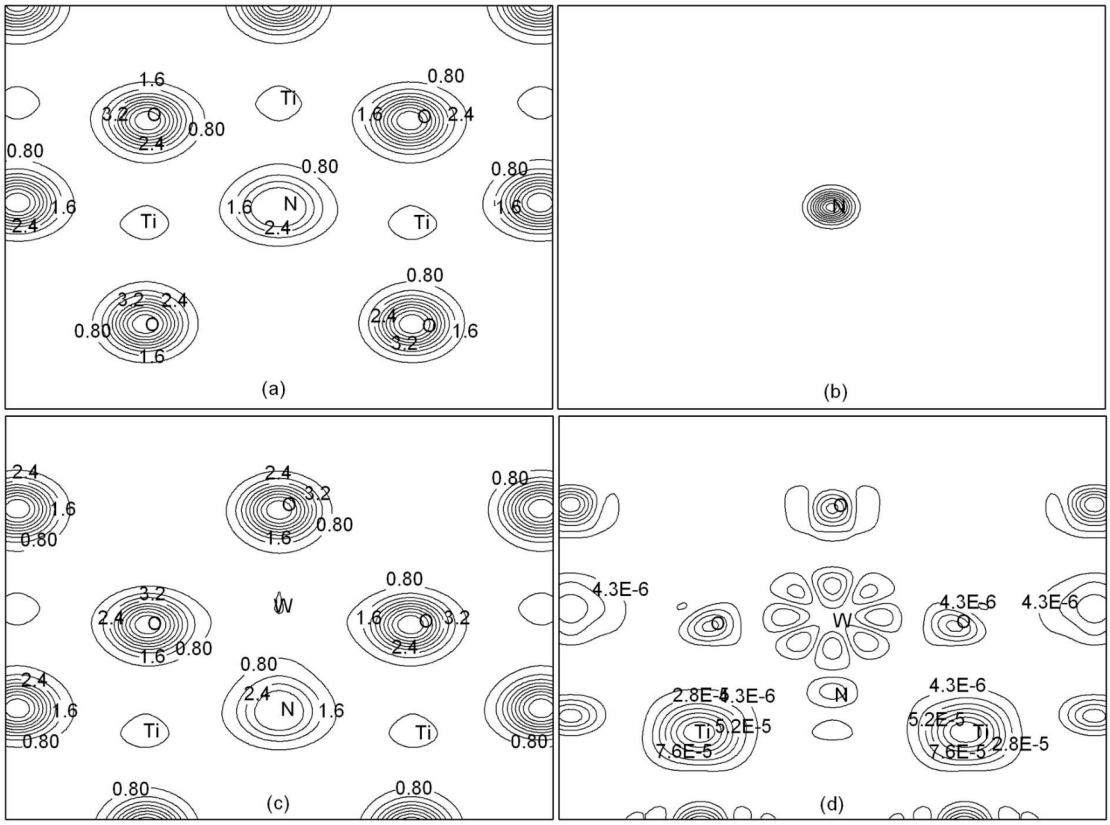
1.6
0.80
Ti
3.2
O
2.4
0.80
1.6
O
2.4
0.80
0.80
0.80
1.6
N
2.4
1.6
2.4
Ti
Ti
0.80
3.2
2.4
0.80
O
2.4
O
1.6
1.6
3.2
(a)
N
(b)
2.4
2.4
0.80
1.6
O
3.2
0.80
0.80
1.6
3.2
0.80
W
2.4
O
1.6
0.80
1.6
O
3.2
2.4
0.80
2.4
N
1.6
2.4
1.6
Ti
Ti
0.80
0.80
0.80
(c)
O
4.3E-6
W
4.3E-6
4.3E-6
O
2.8E-5
4.3E-6
N
4.3E-6
5.2E-5
Ti
5.2E-5
Ti
7.6E-5
7.6E-5
2.8E-5
(d)

Figure 3